Landscape of immune-related signatures induced by targeting of different epigenetic regulators in melanoma: implications for immunotherapy.

Andrea Anichini[1], Alessandra Molla[1], Gabriella Nicolini[1], Valentina E. Perotti[1], Francesco Sgambelluri[1], Alessia Covre[2,3], Carolina Fazio[2], Maria Fortunata Lofiego[2], Anna Maria di Giacomo[2,3], Sandra Coral[2], Antonella Manca[4], Maria Cristina Sini[4], Marina Pisano[4], Teresa Noviello[5,6], Francesca Caruso[5,6], Silvia Brich[7], Giancarlo Pruneri[7,8], Andrea Maurichi[9], Mario Santinami[9], Michele Ceccarelli[5,6], Giuseppe Palmieri[4,10], Michele Maio[2,3*], Roberta Mortarini[1*]

On behalf of the **EP**igenetic **I**mmune-oncology **C**onsortium **A**IRC (**EPICA**) investigators.

[1]Human Tumors Immunobiology Unit, Dept. of Research, [7]Department of Pathology and Laboratory Medicine, [9]Melanoma and Sarcoma Unit, Department of Surgery, Fondazione IRCCS Istituto Nazionale dei Tumori, Milan, Italy. [2]Center for Immuno-Oncology, University Hospital of Siena, Siena, Italy. [3]University of Siena, Siena, Italy. [4]Unit of Cancer Genetics, National Research Council (CNR), Sassari, Italy. [10]University of Sassari, Sassari, Italy. [5]Department of Electrical Engineering and Information Technology (DIETI), University of Naples "Federico II", Naples, Italy. [6]BIOGEM Institute of Molecular Biology and Genetics, Ariano Irpino, Italy. [8]University of Milan, School of Medicine, Italy.

*These authors contributed equally.

Running title: epigenetic drug-mediated immunomodulation in melanoma.

Keywords: melanoma, epigenetic drugs, immune-related signatures, guadecitabine, innate immunity.

Correspondence: Andrea Anichini, PhD, Human Tumors Immunobiology Unit, Dept. of Research, Fondazione IRCCS Istituto Nazionale dei Tumori, Via Venezian 1, 20133 Milan, Italy.

Phone+390223902817. e-mail: andrea.anichini@istitutotumori.mi.it.

Abstract

Background. Innovative cancer immunotherapy approaches aim at combining immune checkpoint inhibitors with other immunomodulatory agents. Epigenetic regulators can control immune-related genes, therefore targeting them with specific inhibitors may be a potential way forward. Here we identified immune-related signatures induced by four classes of epigenetic drugs in human melanoma cells to define the most promising agent and to understand its biological activity in-vitro, in-vivo and in clinical samples.

Methods. Human melanoma cell lines were characterized for mutational and differentiation profile and treated with inhibitors of DNA methyltransferases (guadecitabine), histone deacetylases (givinostat), bromodomain and extraterminal domain proteins (JQ1 and OTX-015) and enhancer of zeste homolog 2 (GSK126). Drug-specific gene signatures were identified by Clariom S and Nanostring platforms. Modulation of 14 proteins was determined by quantitative western blot. Ingenuity Pathway Analysis (IPA) identified Upstream Regulator (UR) molecules explaining changes in gene expression and biological activity of drugs. Gene set enrichment and IPA were used to test modulation of guadecitabine-specific gene and UR signatures, respectively, in on-treatment tumor biopsies from melanoma patients enrolled in the Phase Ib NIBIT-M4 Guadecitabine + Ipilimumab Trial.

Results. Drug-specific gene and UR signatures were identified for each of the four inhibitors. Immune-related genes were frequently upregulated by guadecitabine, to a lesser extent by givinostat, but downregulated by JQ1 and OTX-015. GSK126 was the least active drug. Treatment of melanoma cells with combination of two epigenetic drugs revealed a dominant effect of guadecitabine and JQ1 on immune-related gene modulation. Drug-specific modulatory profiles were confirmed at the protein level. The guadecitabine-specific UR signature was characterized by activated molecules of the TLR, NF-kB, and IFN innate immunity pathways and was induced in drug-treated melanoma, mesothelioma, hepatocarcinoma cell lines and human

melanoma xenografts. Most of the guadecitabine-specific signature genes (n>160) were upregulated in on-treatment tumor biopsies from NIBIT-M4 trial. Progressive activation of guadecitabine UR signature molecules was observed in on-treatment tumor biopsies from responding compared to non-responding patients.

Conclusions. Guadecitabine was the most promising immunomodulatory agent among those investigated. This DNA methyltransferases inhibitor emerged as a strong inducer of innate immunity pathways, supporting the rationale for its use in combinatorial immunotherapy approaches.

Introduction

Following the approval 10 years ago of the anti-CTLA-4 antibody ipilimumab for treatment of metastatic melanoma [1], the management of an increasing spectrum of solid tumors has been revolutionized by the introduction of immunotherapy based on immune checkpoint inhibitors (ICI). Antibodies targeting CTLA-4 or the PD-1/PD-L1 axis have been approved for the treatment of 19 cancer types and two tissue-agnostic conditions [2]. A recent meta-analysis on 23,760 patients and 37 Phase II/III trials, has shown that ICI immunotherapy provides a survival advantage compared to control treatments irrespective of age, sex and ECOG performance status [3]. In spite of these remarkable clinical achievements, only a fraction of patients obtains durable complete responses, even in the most responsive tumor types, and both intrinsic and acquired resistance to ICI is frequent [4]. Therefore, there is an urgent need to design improved immunotherapy approaches. One of the options being tested in early Phase I/II trials is the association of ICIs with immunomodulatory drugs [5,6]. In support of these combinatorial immunotherapy approaches, the recently completed Italian Network for Tumor Biotherapy (NIBIT) Phase Ib NIBIT-M4 trial [6], based on the association of ipilimumab with guadecitabine in advanced melanoma, has shown significant tumor immunomodulatory effects and preliminary evidence of promising clinical activity.

Inhibitors targeting molecules involved in epigenetic regulation have attracted considerable interest in the field of immuno-oncology, as several of these drugs have immune-related effects on tumor cells, as well as on immune cells, that could potentially synergize with ICI [5, 7, 8]. A large series of preclinical studies has shown that epigenetic drugs targeting DNA methyl transferases (DNMT), histone deacetylases (HDAC), enhancer of zeste homolog 2 (EZH2), bromodomain and extra-terminal domain (BET) proteins, and lysine-specific demethylase 1 (LSD-1), when combined with ICI, can contribute to the overall anti-tumor efficacy of immunotherapy,

by affecting the structure of the tumor immune landscape, the generation of anti-tumor immunity, and by modulating immunosuppressive mechanisms and immune escape processes [5, 7, 8]. On the other hand, neither single epigenetic drugs, nor any class of drugs targeting epigenetic regulators, can elicit all of these immunomodulatory effects. Instead, there is a prominent drug-related specificity. For example, DNMT inhibitors can prevent T cell exhaustion [9], activate the interferon response pathway [10], rescue cGAS and STING gene expression [11] and improve antigen processing and presentation [12]. HDAC inhibitors, alone or in association with DNMT inhibitors, can promote T cell recruitment at tumor site [13, 14], reprogram tumor associated macrophages and reduce frequency/suppressive function of Tregs and MDSCs [15, 16]. EZH2 inhibitors can rescue MHC class I transcription [17] and counteract melanoma dedifferentiation [18]. BET inhibitors can downregulate PD-L1 expression [19] and maintain $CD8^+$ T stem cell memory and T central memory differentiation states [20].

The emerging picture is a heterogeneous landscape of diverse and sometimes opposite immune-related activities on either tumors or the tumor microenvironment, or both, by different classes of epigenetic drugs [21, 22]. This immunomodulatory complexity contributes to explain why early combination immunotherapy trials are not focusing on a single epigenetic drug or a drug class. In fact, among >80 recently reviewed Phase I/II combination immunotherapy trials, 15 different inhibitors directed at five classes of epigenetic targets are being tested in association with 9 different ICI [5].

To foster progress in the field of epigenetic immuno-modulation here we carried out a comparative profiling of signatures induced by four epigenetic drugs representing the classes of DNMT, HDAC, BET and EZH2 inhibitors and tested in the melanoma context, a tumor type currently treated by immunotherapy. We defined the breadth of drug-specific immune-related signatures in neoplastic cells fully characterized for genetic background and differentiation profile.

We found that guadecitabine is a strong immunomodulatory agent promoting activation of innate immunity pathways both in-vitro and in-vivo in patients treated with this DNMT inhibitor.

Materials and Methods

Melanoma cell lines. Melanoma cell lines (n=14) were established, maintained and routinely tested for the absence of mycoplasma contamination by PCR, as previously described [23]. Origin of the cell lines from primary lesions (n=1) or from metastases (n=13), histopathological features of the corresponding primary melanoma, cell line authentication by STR profiling (Gene-Print10 kit, Promega) and mutational profile by targeted NGS are described in Table S1A-D. The melanoma cell lines were representative of the main molecular subtypes: $BRAF^{mut}/NRAS^{wt}$ (n=10), $BRAF^{wt}/NRAS^{mut}$ (n=3), and $BRAF^{wt}/ NRAS^{wt}$ (n=1). Expression in n=10 melanoma cell lines of the genes targeted by epigenetic drugs (Fig. S1) was evaluated as described in Supplementary Methods. Mesothelioma cell lines (MPP-89, MM98 and MES2a) were obtained from pleural effusion of mesothelioma patients, cultured, and treated with guadecitabine as previously described [24].

Epigenetic drugs and treatments. Melanoma cell lines were treated with the following drugs: the DNMT inhibitors Decitabine (Selleckchem) and Guadecitabine (MedChemExpress LLC), the HDAC inhibitor Givinostat (ITF-2357, Selleckchem), the BET inhibitors JQ-1 (Selleckchem) and OTX015 (Selleckchem), the EZH2 inhibitor GSK-126 (Selleckchem), and the CDK4/6 inhibitor Abemaciclib (Selleckchem). Susceptibility of ten melanoma cell lines to a range of doses between 7.8 and 3,000 nM of all the drugs was assessed by the 3-(4,5)dimethylthiazol-2,5-diphenyltetrazolium bromide (MTT) assay at 96h as described [25]. On the basis of the dose-response curves, drug doses for all subsequent experiments were tailored for each cell line and for each drug to achieve, in all instances, a response >60% of control in the MTT assay (Table S2A, B). For all subsequent assays, melanoma cells were seeded at $1.25x10^4$/mL in T75 flasks (Greiner Bio-One) with RPMI-1640 medium (Life Technologies Limited) supplemented with 4% FCS (Biological Industries) without antibiotics. Since the activity of epigenetic drugs is coupled to cell proliferation [26], melanoma cells were treated twice with each drug (at T=24h and T=72h) and then evaluated

at T=144h. For some experiments melanoma cells were treated with all possible combinations of two out of the four epigenetic drugs.

NGS analysis. DNA was extracted from 0.5-1x10^6 melanoma cell lines by Purelink Genomic DNA Mini Kit (Invitrogen). RNAse treatment was carried out by RNAse cocktail (Invitrogen). Quantitative assessment of DNA was performed by a Nanodrop 2000 spectrophotometer and DNA integrity was confirmed by gel electrophoresis. Next generation sequencing (NGS) assays on cell lines DNA were done as described in Supplementary Methods.

RNA extraction and gene expression analysis. RNA was extracted from melanoma cell lines by TRIzol (Thermo Fisher Scientific). Melanin removal was carried out by the CTAB-UREA method [27]. Samples were treated with DNase (Qiagen) and purified by RNeasy MinElute Cleanup Kit (Qiagen). The quality of total RNA was first assessed using the RNA 6000 Pico Assay RNA chips run on an Agilent Bioanalyzer 2100 (Agilent Technologies). RNA was also extracted from tumor nodules previously obtained from immunodeficient mice treated or nor with guadecitabine and bearing human melanoma cell line 195 xenografts [28, 29]. Gene expression analysis was performed as described in Supplementary Methods.

Quantitative Western blot. SDS-PAGE was performed with 30 µg of protein lysate on 4–12% NuPAGE Bis-Tris (Thermo Fisher Scientific), in MOPS buffer as described [23]. Primary antibodies (Table S3) were diluted in milk 5% or BSA 5% in TBST as described [23] and incubated overnight. Development was performed with the ECL normal western blot detection system by the chemiluminescence method. Images were acquired with the Alliance Imaging System (Uvitec). Densitometric analysis was carried out by Quantity One software (Bio-Rad Laboratories Inc.). Normalized treated/control ratios were computed on the basis of background-adjusted density values and then visualized by a color code.

Data analysis. The Transcriptomics Analysis Console (TAC) software (Applied Biosystems) was used to identify significantly modulated genes by treatment of two melanoma cell lines

(VRG100 and CST30) treated with Guadecitabine, Givinostat, JQ1, OTX-015, GSK126 or Abemaciclib, and of melanoma nodules removed from immunodeficient mice treated with Guadecitabine. Analysis settings were as follows: gene level fold change >|1.2|, gene-level p value: <0.05; gene-level FDR: <0.05. Nanostring data were analyzed with nSolver software 4.0 (Nanostring Technologies) as described in Supplementary Methods. VENNTURE software [30], allowing Edwards-Venn diagram generation for multiple dataset analysis, was used to classify all genes with significant modulation by any of the treatments. Ingenuity Pathway Analysis (IPA 8.5, www.ingenuity.com) was used, as described in Supplementary Methods, to carry out Upstream Regulator (UR) analysis on: a) significantly modulated genes by different treatments; b) differentially expressed genes in pre-therapy and on-treatment lesions from responding vs non responding patients from the NIBIT-M4 trial [6]. IPA was also used for canonical pathway analysis as described in Supplementary Methods. RNA-seq and DNA methylation data from tumor samples obtained at baseline (week 0), at week 4 and week 12 of treatment were retrieved from the published NIBIT M4 Phase Ib trial [6]. Raw data as FASTQ files of melanoma patient's biopsies were aligned to the human reference genome (GRCh38/hg38) using STAR version 2.7.0b [31] and the gene expression level was quantified using featureCounts version 1.6.3 [32]. Downstream analyses were performed in the R statistical environment. EDASeq package [33] was used to normalize the count matrix using GC-correction for the within normalization step and upper-quantile for the between phase. EdgeR package [34] was used to identify differentially expressed genes at week4 and week12 compared to week0 and at week12 compared to week4. The guadecitabine-specific gene signature (upregulated genes), identified in this manuscript, was used to construct a heatmap of the Log2 fold changes for the three different comparisons. ClusterProfiler package [35] was used to perform and visualize GSEA pre-ranked analyses using the guadecitabine-specific gene signature in each comparison.

Results

Epigenetic drugs modulate expression of 20 gene families. A panel of melanoma cell lines was fully characterized for tissue of origin (Table S1A), expression of epigenetic drug targets (Fig. S1), mutational profile (Table S1D), differentiation-related signatures (Fig. S2) as defined by Tsoi et al [36], as well as for susceptibility to four epigenetic drugs (Fig. S3 and Table S2A, B). Two of these cell lines (VRG100 and CST30) were selected as examples of divergent transcriptomic profiles found in melanoma (Fig. S4). Gene modulation in these two lines by DNMT (decitabine/guadecitabine), HDAC (givinostat), BET (JQ1) and EZH2 (GSK126) inhibitors was investigated by whole genome gene expression analysis. The CDK4/6 inhibitor abemaciclib, a drug with immunomodulatory activity unrelated to epigenetic regulation [37], was also included in these experiments. The five drugs modulated 6% to >30% of the genes in the two cell lines (Fig. S5) and, based on Edwards-Venn diagrams [30], showed both drug-specific as well as shared modulatory activities (Fig. S6). Guadecitabine, givinostat, JQ1, GSK-126 and abemaciclib exerted pleiotropic modulatory activities on 20 gene families grouped into 7 biological functions (Fig. 1), including epigenetic regulation, proliferation, immune regulation, enzymatic activity, structural function, adhesion and cellular differentiation. The drugs elicited variable modulatory activity on epigenetic regulator genes (DNMT, HDAC, BET and PRC2 components), and on genes encoding histones and nuclear pore complex interacting proteins (NPIPA genes). Guadecitabine, givinostat and JQ1 were the most active drugs, followed by GSK-126, in modulation of genes encoding HLA-I/II and antigen processing machinery (APM) components, heat shock proteins, IFN (IFI and IRF), TNF/TNFR and TGFβ pathways. These immune-related genes were frequently upregulated by guadecitabine and givinostat, but downregulated by JQ1 (Fig. 1).

Guadecitabine is the most active drug in upregulation of immune-related genes, while JQ1 is a strong suppressor of immune-related gene expression. Immunomodulation emerged as a dominant feature of the epigenetic drugs in the two cell lines VRG100 and CST30. Therefore, we

focused on the quantitative determination of 731 immune-related genes, present in the Nanostring Cancer Immune panel and re-classified by us into 21 functional classes (Fig. S7). In these experiments we used the whole panel of melanoma cell lines. Quantitative analysis (Fig. S8) and hierarchical clustering of Nanostring data, according to the 21 functional classes (Fig. S9), indicated that guadecitabine and givinostat had a predominantly positive effect on immune-related gene expression, while JQ1 induced frequent gene downmodulation. To reduce the complexity emerging from the gene-level analysis (shown in Table S4) of the modulatory effects of all drugs on the 21 functional classes, we used *ad-hoc* developed metrics. This approach (Fig. 2) allowed to visualize the proportion of genes being significantly modulated in each gene class and the direction of the most frequent effects by each drug (in terms of up- or down-regulated genes). Guadecitabine and givinostat mostly induced upregulation of immune-related genes in the majority of the cell lines, while the BET inhibitor JQ1 produced the opposite effects (Fig. 2). GSK126 and abemaciclib were the least active drugs and also showed cell line-specific effects. Immune-related gene modulation by the three most active drugs was observed across the melanoma cell line panel without any clear association with the mutational or differentiation profile of the cell lines (Fig. 2). Two of the cell lines (BNV13 and GRD43) were treated with decitabine, the active metabolite of guadecitabine, yielding similar results to the cell lines treated with guadecitabine (Fig. 2). Guadecitabine was the most active drug in upregulation of genes belonging to the following functional classes: cancer testis, adhesion molecules, positive/negative co-stimulation, myeloid-related, cytokines and receptors, T/NK related, immune cell lineage/differentiation, regulation of inflammation, TNF/TNFR pathway, Type I-II-III IFN pathways and intracellular signaling (Fig. 2 and Table S4 for gene level analysis). The BET inhibitor JQ1 was the most active drug in inducing downregulation of selected genes related to immune cells lineage/differentiation markers, TNF/TNFR pathway, Type I-II-III IFNs pathways, intracellular signaling and transcriptional regulation, TLR pathway, HLA Class I/II and antigen presentation

pathways (Fig. 2 and Table S4 for gene-level analysis). Nanostring analysis of a subset of six cell lines treated with a different BET inhibitor (OTX-015), tested in clinical trials [38], confirmed the predominant down-modulation of immune-related genes by this class of epigenetic drugs (Fig. S10).

By exploiting Nanostring data from all cell lines we derived all the epigenetic drug-specific gene signatures listing the most frequently modulated genes (Fig. S11). The guadecitabine-specific and the JQ1-specific gene signatures contained each ~170 genes, mostly being upregulated by the former drug while being downregulated by the latter. The givinostat-specific gene signature contained 128 genes (several shared with the guadecitabine signature) while the GSK126 signature contained 40 genes (Fig S11).

Combinatorial treatments with epigenetic drugs indicate a dominant effect of guadecitabine and JQ1 on immune-related gene modulation. Melanoma cells from the panel were treated with all six binary combinations of the four epigenetic drugs (guadecitabine + givinostat, guadecitabine + JQ1, guadecitabine + GSK126, givinostat + JQ1, givinostat + GSK126, JQ1 + GSK126). Gene modulation induced by the combinations was then measured by Nanostring Cancer Immune panel and compared to the effects of single drugs (Table S5). In most instances, combinatorial treatments did not enhance gene modulation compared to single treatments. Moreover, the effect of a “dominant” drug was evident. In fact, association of guadecitabine with givinostat or with GSK-126 replicated the pattern of immune-related gene upregulation exerted by guadecitabine alone (Table S5). Similarly, any association of JQ1 with the other drugs replicated the dominant suppressive effect on immune-related gene expression exerted by JQ1 alone (Table S5). These results argue against the possibility of achieving more effective modulation of immune-related genes by combining two epigenetic drugs belonging to different classes.

Immune-related genes modulated by guadecitabine belong to the "low expression/high methylation" class. Guadecitabine is expected to induce upregulation of genes subjected to negative regulation by promoter methylation [39]. Therefore genes in the guadecitabine signature should be characterized by high levels of methylation and low expression. To test this hypothesis, we retrieved data on gene expression and DNA methylation of a large set of melanoma cell lines from the CellMinerCDB database [40]. We defined a gene expression/methylation classification in 4 subsets (a,b,c and d in Fig. S12A-C) by setting appropriate methylation and expression thresholds. Then this classification was extended to all the genes in the guadecitabine-specific signature (Fig. S13). We found that most of them were indeed characterized by high methylation and low expression in most cell lines, namely they belong to group b). We then retrieved gene-specific methylation and gene expression data previously obtained on tumor samples obtained at week 0 (baseline, w0), at week 4 (w4) and week 12 (w12) in the context of the guadecitabine + ipilimumab NIBIT-M4 clinical trial [6]. We focused on the subset of the cancer testis (CT) genes , that can be modulated by guadecitabine and that have tumor-restricted expression [41]. By adopting a scoring system described in Fig. S14 A, B, we found frequent increased expression of CT genes associated with reduction of their methylation level in tumor samples obtained at w4 and w12 of treatment, compared to w0 biopsies (Fig. S14C).

Epigenetic drugs modulate expression of immune-related proteins in melanoma. The immuno-related activity of the epigenetic drugs was assessed by quantitative Western blot analysis (pipeline of data analysis and visualization described in Fig. S15 and Fig. S16) by looking at expression and modulation of 14 immune-related and differentiation-related proteins in 11 melanoma cell lines (Fig. 3). Guadecitabine, followed by givinostat and GSK-126, were the most active drugs in increasing expression of HLA class I and II-related proteins (HLA Class I heavy chain, B2M and HLA-DR), but guadecitabine was more active compared to givinostat and to GSK-126 on molecules belonging to the antigen processing and presentation pathway (TAP1, TAP2,

LMP2/PSMB9, Fig. 3). In contrast, the two BET inhibitors induced, in most instances, a reduction of expression of these classes of proteins. Guadecitabine and the BET inhibitors confirmed their opposite effects on expression of IFN-pathway related proteins (OAS3 and IFITM1), on PD-L1 / CD274 and on CEACAM1. Interestingly, all the 5 epigenetic drugs had a predominant inhibitory effect on expression of melanoma differentiation-related proteins MITF and SOX-10 and of the transcription factor MYC (Fig. 3).

Upstream Regulator (UR) analysis identifies activation of innate immunity and of inflammation-related pathways as the main immune-related activity of guadecitabine. To gain insight into the biological activity of the different epigenetic agents we used UR analysis, by IPA. UR analysis (pipeline of data analysis described in Fig. S17) is a computational tool that identifies the upstream transcriptional regulators that control downstream genes and explain the observed gene expression changes in the dataset. UR analysis also predicts the functional status (activated or inhibited) of each UR molecule. Each of the predicted UR can be associated with the main cellular processes and pathways it belongs, thus allowing to improve understanding of the overall biological activity of each drug (Fig. S17).

UR analysis, based on p values and activation Z scores (Table S6) and applied to gene expression dataset of cell lines VRG100 and CST30, confirmed the wide range of biological activities of all drugs. Several of the significant URs were molecules involved in immune-regulation (highlighted in green in Table S6). These UR molecules were often predicted to be activated by guadecitabine, and to a lesser extent by givinostat, but frequently inhibited by JQ1 or by GSK126. To provide a direct comparison of all drugs at the UR level, significantly modulated URs by at least two different inhibitors were grouped and visualized according to 18 functional groups (Fig. S18 and Fig. S19 dealing with cell lines VRG100 and CST30, respectively). This analysis revealed not only the breadth and drug-related specificity of epigenetic drug activity, but even the differences

among these drugs (i.e. the UR with opposite activation status). A large set of these URs (group 12 in Fig. S18 and group 14 in Fig. S19) were immunity/inflammation-related molecules belonging to at least seven functional groups/pathways (cytokines, IFNs, JAK-STAT, IRFs, TLR, NF-kB, TNF) frequently activated by guadecitabine, and to a lesser extent by givinostat, while almost invariably predicted to be inhibited by JQ1. Scatter plots of significantly modulated URs by guadecitabine vs JQ1, in cell line VRG100, confirmed the opposite biological activity of these two drugs (Fig. S20A). In fact, a large set of URs activated by guadecitabine were inhibited by JQ1. In contrast, scatter plots comparing URs modulated by guadecitabine and givinostat revealed a set of URs activated by both drugs, as well as URs activated only by guadecitabine (Fig. S20B).

The UR analysis was then extended to the whole panel of cell lines using Nanostring data as input and by focusing on the activity of guadecitabine. By such analysis we identified 51 activated URs (z score >2) and 9 inhibited URs (Z score <-2) by guadecitabine in the majority of cell lines (i.e. $\geq$ 6/10 cell lines, Fig. 4A). Additional 36 URs were predicted to be activated in a subset of the cell lines (i.e. 5/10 cell lines, Fig. 4B). To visualize the overall biological activity of guadecitabine the URs were labeled with color-coded arrows pointing to the pathways/biological processes these molecules belong. On this basis, the main immune-related activity of guadecitabine could be summarized as an activator of innate immunity (NF-kB, TLR and Type I-III IFN) and inflammation-related pathways (Fig. 4A, B).

We then tested whether the guadecitabine-specific UR signature could be induced by this drug in different cellular contexts, beyond the melanoma histotype, as well as in tumor nodules from a previously described [28,29] in-vivo model. By gene expression analysis in mesothelioma cell lines treated with guadecitabine and by retrieving published gene expression data of hepatocarcinoma cell lines treated with this drug [42], we found that guadecitabine-specific UR signature molecules were predicted to be activated (color-coded dots in Fig. 5A, B). Several of the

guadecitabine-specific URs activated by this drug in-vitro in cell lines were also activated in-vivo in tumor nodules from immunodeficient mice bearing a human melanoma cell line xenograft [28,29] and treated with guadecitabine (Fig. S21A). In addition, canonical pathway analysis by IPA, indicated that several genes in the IFN-γ and IFN-α/β pathways were significantly upregulated by guadecitabine in the tumor xenografts (Fig. S21B). Taken together, these results indicate that guadecitabine is a strong inducer of innate immunity pathways and that its biological function can be consistently detected not only in-vitro, irrespective of tumor mutational background and histotype, but even in-vivo.

The guadecitabine-specific gene and UR signatures are induced in-vivo in on-treatment tumor biopsies from NIBIT-M4 patients. Modulation of genes belonging to the guadecitabine-specific signature was investigated by retrieving RNA-seq data of pre-therapy (w0), and on-treatment (w4 and w12) melanoma biopsies from patients enrolled in the NIBIT-M4 trial [6]. Different groups of guadecitabine-specific signature genes (highlighted by vertical color bars in Fig. 6A) showed increased expression in w12 or w4 on-treatment samples compared to baseline or in w12 compared to w4 biopsies. Overall, almost 92% of the guadecitabine-specific signature genes were upregulated in biopsies obtained at w12 or w4, compared to w0 (Fig. 6A). By gene set enrichment analysis [43] the guadecitabine-specific gene signature showed a significant increase at w12 compared to w4 and w0, but not at w4 compared to w0 (Fig. 6B-D). We then asked whether treatment in monotherapy with the anti-CTLA-4 mAb could also lead to upregulation of most of the guadecitabine signature genes in on-treatment lesions. In two published datasets [44, 45] involving n=45 [44] and n=54 melanoma patients [45], among 376 and 286 genes upregulated by Ipilimumab in on treatment lesions compared to baseline, we found only 35/166 (21.1%) and 28/166 genes (16.9%) of the guadecitabine signature, respectively (data not shown).

We then identified genes showing differential expression, at each time point, in biopsies from responding vs non-responding patients of the NIBIT–M4 trial and then we subjected these differentially expressed genes to UR analysis by IPA. The results revealed progressive activation of several guadecitabine-specific UR signature molecules in on-treatment (w4 and w12) tumor biopsies from responding compared to non-responding patients (Fig. 7A, B), as well as a strong correlation of these activated UR at w4 vs w12 tumor samples (Fig. 7C).

Taken together these results strongly support the notion that the guadecitabine-specific gene signature defined in-vitro in melanoma cell lines can be modulated even in-vivo at tumor site in patients treated with this DNMT inhibitor. Moreover, the progressive activation of the UR signature in responding vs non responding patients suggests that the clinical activity of guadecitabine in melanoma patients depends on effective activation of innate immunity pathways.

Discussion

Characterization of the biological activity of the four investigated agents targeting distinct epigenetic regulators by gene expression, quantitative western blot and UR analyses in melanoma cell lines, indicated that the DNMT inhibitor guadecitabine and the BET inhibitor JQ1 were the most active drugs, but exerted opposite immuno-regulatory functions. Comparison of the drug-specific immune-related gene signatures indicated that guadecitabine upregulated several genes in each of the 21 functional classes present on the Nanostring Cancer Immune panel, while JQ1 predominantly downregulated genes in such classes. Moreover, almost all immune-related URs predicted to be activated by guadecitabine were instead inhibited by JQ1 in the majority of the melanoma cell lines tested. Among UR predicted to be inhibited by JQ1 we found not only molecules belonging to the IFN-gamma pathway, known to be targeted by this BET inhibitor [46], but also molecules belonging to the TLR and NF-kb pathways regulated by the BET proteins [21]. The experiments looking at gene modulation in melanoma cell lines, by treatment with combinations of two different epigenetic inhibitors, confirmed that the guadecitabine and JQ1 were the dominant drugs that determined opposite responses to treatment, irrespective of the other drug used in the combination. Collectively, the results suggest that guadecitabine elicits marked pro-inflammatory effects, while JQ1 is mainly an anti-inflammatory drug.

The breadth of non-immuno-related effects of the four epigenetic inhibitors emerged through comparative transcriptomic analysis. The four drugs had a variable impact on expression of genes encoding DNMT, HDAC, histones, BET, and PRC2 components. This suggests that drug activity of these agents is not uniquely dependent on inhibition of their specific targets, but even on modulation of additional genes which contribute to different aspects of epigenetic regulation. The drugs affected also expression of genes encoding proteolytic enzymes (cathepsins), and their inhibitors (serpins), thus implicating epigenetic drugs in the regulation of different cancer-related processes, controlled by cathepsins, such as proliferation, angiogenesis, metastasis and invasion.

Taken together, these results significantly extend previous knowledge on non-immuno-related anti-tumor activities of epigenetic inhibitors, such as reactivation of tumor suppressor genes by demethylating agents [47], promotion of cell death and suppression of angiogenesis by HDAC inhibitors [48], inhibition of proto-oncogenes MYC and BCL2 by BET inhibitors [49] and downregulation of DNA repair genes by EZH2 inhibitors [50].

In depth analysis of guadecitabine biological activity indicated that this DNMT inhibitor upregulated genes belonging to 21 immune-related classes. The >160-gene drug-specific signature of guadecitabine and the related UR signature profiled the remarkable immunomodulatory activity of this drug. The emerging immune-related biological activity of guadecitabine, identified through UR analysis, was consistently observed across a panel of melanoma cells lines with widely divergent mutational and differentiation profiles, as well as across different tumor histotypes. A pre-clinical tumor model confirmed the activation of the guadecitabine-specific UR signature even in-vivo. Finally, we found that most of the guadecitabine-specific signature genes were upregulated at w4 or w12 in clinical samples from NIBIT-4 patients, but not in on treatment tumor samples from patients treated with Ipilimumab only [44-45]. Moreover, progressive activation of the guadecitabine-specific UR signature could distinguish on treatment tumor biopsies of responding compared to non-responding patients. These results suggest that the clinical efficacy of guadecitabine in melanoma patients is strictly associated with the effective promotion, in-vivo, of the innate immunity pathways that define the biological activity of this DNMT inhibitor.

In conclusions, the findings of this study support a mechanistic rationale for development of combinatorial immune intervention where boosting of NF-kB, TLR, Type I-III IFN and inflammation-related pathways by the DNMT inhibitor guadecitabine may cooperate with rescue of adaptive immunity by immune checkpoint blockade to improve efficacy of cancer immunotherapy.

Abbreviations.

APM: antigen processing machinery; BET: bromodomain and extra-terminal domain; CT: cancer testis; DNMT: DNA methyltransferases; EZH2: enhancer of zeste homolog 2; HDAC: histone deacetylases; ICI: immune checkpoint inhibitor; IPA: Ingenuity Pathway Analysis; LSD-1: Lysine-specific demethylase 1; MTT: 3-(4,5)dimethylthiazol-2,5-diphenyltetrazolium bromide; NIBIT: Italian Network for Tumor Biotherapy; NGS: next generation sequencing; TAC: Transcriptomic Analysis Console; UR: Upstream Regulator.

Supplementary Information.

-Supplementary Methods and Figures.pdf. This file contains supplementary materials and methods and supplementary figures S1 to S21. **-Fig. S1**. Expression in ten melanoma cell lines of genes and gene families targeted by epigenetic drugs. **-Fig. S2**. Melanoma differentiation profile of cell lines according to expression of seven subtype signatures and four main melanoma subsets. **-Fig. S3.** Susceptibility of ten melanoma cell lines to the anti-proliferative effects of epigenetic drugs. **-Fig. S4.** Volcano plot of differentially expressed genes in VRG100 and CST30 cell lines. **-Fig. S5.** Whole genome gene modulation analysis by epigenetic drugs in two melanoma cell lines. -**Fig. S6.** Edwards-VENN diagram analysis of significantly modulated genes. **-Fig. S7.** Original and revised gene classification of the NanoString nCounter PanCancer Immune Profiling panel. **-Fig. S8.** Quantitative analysis of Nanostring data in ten melanoma cell lines treated with epigenetic drugs. **-Fig. S9.** Modulation of immune-related genes in melanoma cell lines by epigenetic drugs. **-Fig. S10.** Comparison of immune-related gene modulation by BET inhibitors JQ1 and OTX-015. -**Fig. S11.** Immune-related signatures of epigenetic drugs in melanoma. **-Fig. S12.** Expression/methylation relationship, for selected genes in the guadecitabine-specific gene signature, among melanoma cell lines present in the GDSC-MGH Sanger database. **-Fig. S13.** Expression/methylation relationship of genes belonging to the guadecitabine-specific signature

according to the GDSC-MGH Sanger melanoma dataset. **-Fig. S14.** Changes in gene expression and gene methylation for the cancer testis class of genes in tumor biopsies from melanoma patients enrolled in the NIBIT-M4 trial. **-Fig. S15.** Outline of the strategy for quantitative analysis and visualization of western blot data. **-Fig. S16.** Quantitative western blot analysis and visualization of the modulation of LMP7 by epigenetic drugs in 11 melanoma cell lines. **-Fig. S17.** Pipeline of data analysis based on Upstream Regulators (UR) identified by IPA. **-Fig. S18.** Classification of URs significantly modulated by at least two different drugs in melanoma cell line VRG100. **-Fig. S19.** Classification of URs significantly modulated by at least two different drugs in melanoma cell line CST30. **-Fig. S20.** Comparison of all URs predicted to be activated or inhibited by Guadecitabine vs JQ1 and by Guadecitabine vs Givinostat. **-Fig. S21.** Comparison of URs activated by guadecitabine in-vitro and in-vivo.

-Table S1.xlsx. Origin of melanoma cell lines, histopathological features of the corresponding primary tumor, cell line authentication data by STR profiling, and mutational profile by NGS of 14 melanoma cell lines used in this study.

-Table S2.xlsx. Drug doses used for experiments and effect of each drug at such dose in the MTT assay on each cell line.

-Table S3.xlsx. Antibodies used in quantitative western blot analysis.

-Table S4.xlsx. Modulation of immune-related genes belonging to 21 functional classes by epigenetic drugs. This excel file has 21 sheets.

-Table S5.xlsx. Immune-related gene modulation by epigenetic drugs and by combinatorial treatments. This excel file has 5 sheets.

-Table S6.xlsx. Upstream Regulator analysis on differentially expressed genes in drug-treated vs untreated cell lines VRG100 and CST30.

Declarations

Ethics approval and consent to participate. The data analyzed during this study concern gene expression and methylation in tumor samples from the published NIBIT-M4 trial [6]. The NIBIT-M4 Phase Ib trial was conducted in accordance with the ethical principles of the Declaration of Helsinki and the International Conference on Harmonization of Good Clinical Practice. The protocol was approved by the independent ethics committee of the University Hospital of Siena (Siena, Italy). All participating patients (or their legal representatives) provided signed-informed consent before enrolment. The trial was registered with European Union Drug Regulating Authorities ClinicalTrials EudraCT, number 2015-001329-17, and with ClinicalTrials.gov, number NCT02608437.

Consent for publication. Not applicable.

Availability of data and materials. The datasets generated during the current study are available in the Gene Expression Omnibus (GEO) repository with the following GEO accession numbers: GSE189628, GSE189629, GSE189630, GSE189631. The data analyzed during this study concerning gene expression and methylation in tumor samples from patients enrolled in the published NIBIT-M4 trial were retrieved from ref. 6.

Competing interests. AA has received compensated educational activities from Bristol-Myers Squibb. AMDG has served as a consultant and/or advisor to Incyte, Pierre Fabre, Glaxo Smith Kline, Bristol-Myers Squibb, Merck Sharp Dohme, and Sanofi and has received compensated educational activities from Bristol Myers Squibb, Merck Sharp Dohme, Pierre Fabre and Sanofi. MM has served as a consultant and/or advisor to Roche, Bristol-Myers Squibb, Merck Sharp Dohme, Incyte, AstraZeneca, Amgen, Pierre Fabre, Eli Lilly, Glaxo Smith Kline, Sciclone, Sanofi, Alfasigma, and Merck Serono; and owns shares in Epigen Therapeutics. SC and AC own shares in Epigen Therapeutics. G.Palmieri has advisory role for Bristol-Myers Squibb, Merck Sharp Dohme, Roche,

Novartis, Pierre-Fabre, Incyte. A.Maurichi has received compensated educational activities from Novartis. G.Pruneri has received meetings honoraria from from AstraZeneca, Novartis, Exact Sciences, Roche and Illumina and is advisory board member of ADS Biotec. A.Molla, GN, VEP, FS, CF, MFL, A.Manca, MCS, MP, SB, TN,FC, MS and RM declare no conflicts of interests.

Funding. The research leading to these results has received funding from: AIRC under 5 per mille 2018 – ID.21073 program – P.I. Maio Michele, Group Leader Anichini Andrea and Ministry of Health, Lombardy and Tuscany regions, Bando Ricerca Finalizzata, grant number NET-2016-02361632, P.I. Michele Maio.

Authors' contributions AA: conceptualization, funding acquisition, resources, supervision, data curation, formal analysis, visualization, methodology, writing of original draft. A.Molla: cell biology experiments, methodology, data curation. GN: molecular biology experiments, methodology, data curation. VEP: western blot experiments, methodology, formal analysis, data curation. FS: cell biology experiments, methodology, visualization, data curation. AC: data curation, methodology, writing–review and editing. CF: in-vivo and in-vitro experiments, methodology, data curation. MFL: in-vivo and in-vitro experiments, methodology, data curation. AMDG: data curation, resources, writing–review and editing. SC: Project administration, data curation, resources. A.Manca: NGS experiments, methodology, data analysis and curation. MCS: NGS experiments, data analysis and curation, methodology. MP: NGS experiments, methodology, data analysis and curation. TN: data analysis; FC: data analysis. SB: Nanostring experiments, methodology, data curation. G.Pruneri: resources, writing–review and editing. A.Maurichi: data curation, writing–review and editing. MS: data curation, writing–review and editing. MC: conceptualization, data analysis, writing–review and editing. G.Palmieri: conceptualization, funding acquisition, data curation, resources, formal analysis. MM: conceptualization, funding acquisition, data curation, resources, writing–review and editing. RM: conceptualization, supervision, data analysis and curation, writing of original draft.

564 **Acknowledgements.** The authors wish to tank the **EP**igenetic **I**mmune-oncology **C**onsortium **A**IRC
565 (**EPICA**) investigators (Daniela Massi, Ulrich Pfeffer) for helpful discussion of data and critical
566 review of the manuscript.

567

568

569

570

571

572

573

574

575

576

577

578

579

580

581

582

583

584

585

586

587

588

References

1. Hodi FS, O'Day SJ, McDermott DF, Weber RW, Sosman JA, Haanen JB, et al. Improved survival with ipilimumab in patients with metastatic melanoma. N Engl J Med. 2010;363:711-23.
2. Twomey JD, Zhang B. Cancer immunotherapy update: FDA-approved checkpoint inhibitors and companion diagnostics. AAPS J. 2021;23:39.
3. Yang F, Markovic SN, Molina JR, Halfdanarson TR, Pagliaro LC, Chintakuntlawar AV, et al. Association of sex, age, and eastern cooperative oncology group performance status with survival benefit of cancer immunotherapy in randomized clinical trials a systematic review and meta-analysis. JAMA Netw Open. 2020;3:e2012534.
4. Sharma P, Hu-Lieskovan S, Wargo JA, Ribas A. Primary, adaptive, and acquired resistance to cancer immunotherapy. Cell. 2017;168:707-23.
5. Topper MJ, Vaz M, Marrone A, Brahmer JR, Baylin SB. The emerging role of epigenetic therapeutics in immuno-oncology. Nat Rev Clin Oncol. 2020;17:75-90.
6. Di Giacomo AM, Covre A, Finotello F, Rieder D, Danielli R, Sigalotti L, et al. Guadecitabine plus Ipilimumab in unresectable melanoma: the NIBIT-M4 clinical trial. Clin Cancer Res. 2019;25:7351-362.
7. Aspeslagh S, Morel D, Soria JC. Postel-Vinay S. Epigenetic modifiers as new immunomodulatory therapies in solid tumours. Ann Oncol. 2018;29:812–24.
8. Jones PA, Ohtani H, Chakravarthy A, De Carvalho DD. Epigenetic therapy in immune-oncology. Nat Rev Cancer. 2019;19:151-61.
9. Ghoneim HE, Fan Y, Moustaki A, Abdelsamed HA, Dash P, Dogra P, et al. De novo epigenetic programs inhibit PD-1 blockade-mediated T cell rejuvenation. Cell. 2017;170:142-57.

10. Chiappinelli KB, Strissel PL, Desrichard A, Li H, Henke C, Akman B, et al. Inhibiting DNA methylation causes an interferon response in cancer via dsRNA including endogenous retroviruses. Cell. 2015;162:974–86.
11. Falahat R, Berglund A, Putney RM, Perez-Villarroel P, Aoyama S, Pilon-Thomas S, et al. Epigenetic reprogramming of tumor cell–intrinsic STING function sculpts antigenicity and T cell recognition of melanoma. Proc Natl Acad Sci USA. 2021;118:1-9.
12. Luo N, Nixon MJ, Gonzalez-Ericsson PI, Sanchez V, Opalenik R, Li H, et al. DNA methyltransferase inhibition upregulates MHC-I to potentiate cytotoxic T lymphocyte responses in breast cancer. Nat Commun. 2018;9:248.
13. Topper MJ, Vaz M, Chiappinelli KB, DeStefano Shields CE, Niknafs N, Yen CR, et al. Epigenetic therapy ties MYC depletion to reversing immune evasion and treating lung cancer. Cell. 2017;171:1284–300.
14. Zheng H, Zhao W, Yan C, Watson CC, Massengill M, Xie M, et al. HDAC inhibitors enhance T-cell chemokine expression and augment response to PD-1 immunotherapy in lung adenocarcinoma. Clin Cancer Res. 2016;22:4119–32.
15. Xiaolei Li X, Su X, Liu R, Pan Y, Fang J, Cao L, et al. HDAC inhibition potentiates anti-tumor activity of macrophages and enhances anti-PD-L1-mediated tumor suppression. Oncogene. 2021;40:1836–850.
16. Orillion A, Hashimoto A, Damayanti N, Shen L, Adelaiye-Ogala R, Arisa S, et al. Entinostat neutralizes myeloid-derived suppressor cells and enhances the antitumor effect of PD-1 inhibition in murine models of lung and renal cell carcinoma. Clin Cancer Res. 2017;23:5187–201.
17. Burr ML, Sparbier CE, Chan KL, Chan Y, Kersbergen A, Lam EYN, et al. An evolutionarily conserved function of polycomb silences the MHC class I antigen presentation pathway and enables immune evasion in cancer. Cancer Cell. 2019;36:385-401.

18. Zingg D, Arenas-Ramirez N, Sahin D, Rosalia RA, Antunes AT, Haeusel J, et al. The histone methyltransferase Ezh2 controls mechanisms of adaptive resistance to tumor immunotherapy. Cell Rep. 2017;20:854-67.

19. Hogg SJ, Vervoort SJ, Deswal S, Ott CJ, Li J, Cluse LA, et al. BET-Bromodomain inhibitors engage the host immune system and regulate expression of the immune checkpoint ligand PD-L1. Cell Rep. 2017;18:2162–174.

20. Kagoya Y, Nakatsugawa M, Yamashita Y, Ochi T, Guo T, Anczurowski M, et al. BET bromodomain inhibition enhances T cell persistence and function in adoptive immunotherapy models. J Clin Invest. 2016;126:3479–494.

21. Wang N, Wu R, Tang D, Kang R. The BET family in immunity and disease. Signal Transduct Target Ther. 2021;6:23.

22. Fazio C, Covre A, Cutaia O, Lofiego MF, Tunici P, Chiarucci C, et al. Immunomodulatory properties of DNA hypomethylating agents: selecting the optimal epigenetic partner for cancer immunotherapy. Front Pharmacol. 2018;9:1443.

23. Perotti V, Baldassari P, Molla A, Nicolini G, Bersani I, Grazia G, et al. An actionable axis linking NFATc2 to EZH2 controls the EMT-like program of melanoma cells. Oncogene. 2019;38:4384-396.

24. Sigalotti L, Coral S, Altomonte M, Natali L, Gaudino G, Cacciotti P, et al. Cancer testis antigens expression in mesothelioma: role of DNA methylation and bioimmunotherapeutic implications. Br J Cancer. 2002;86:979–82.

25. Grazia G, Vegetti C, Benigni F, Penna I, Perotti V, Tassi E, et al. Synergistic anti-tumor activity and inhibition of angiogenesis by cotargeting of oncogenic and death receptor pathways in human melanoma. Cell Death Dis. 2014;5:e1434.

661 26. Cheng Y, He C, Wang M, Ma X, Mo F, Yang S, et al. Targeting epigenetic regulators for
662 cancer therapy: mechanisms and advances in clinical trials. Signal Transduct Target Ther.
663 2019;4:62.
664 27. Lagonigro MS, De Cecco L, Carninci P, Di Stasi D, Ranzani T, Rodolfo M, et al. CTAB-urea
665 method purifies RNA from melanin for cDNA microarray analysis. Pigment Cell Res.
666 2004;17:312-15.
667 28. Coral S, Sigalotti L, Colizzi F, Spessotto A, Nardi G, Cortini E, et al. Phenotypic and functional
668 changes of human melanoma xenografts induced by DNA hypomethylation:
669 Immunotherapeutic implications. J Cell Physiol. 2006;207:58-66.
670 29. Covre A, Coral S, Di Giacomo AM, Taverna P, Azab M, Maio M. Epigenetics meets immune
671 checkpoints. Semin in Oncol. 2015;42:506-13.
672 30. Martin B, Chadwick W, Yi T, Park S, Lu D, Ni B, et al. VENNTURE–a novel venn diagram
673 investigational tool for multiple pharmacological dataset analysis. Plos One.
674 2012;7:e36911.
675 31. Dobin A, Davis CA, Schlesinger F, Drenkow J, Zaleski C, Jha S, et al. STAR: ultrafast
676 universal RNA-seq aligner. Bioinformatics. 2013;29:15–21.
677 32. Liao Y, Smyth GK, Shi W. FeatureCounts: an efficient general purpose program for assigning
678 sequence reads to genomic features. Bioinformatics. 2013;30:923-30.
679 33. Risso D, Schwartz K, Sherlock G, Dudoit S. GC-Content Normalization for RNA-Seq Data.
680 BMC Bioinformatics. 2011;12:480.
681 34. Robinson MD, McCarthy DJ, Smyth GK. EdgeR: a Bioconductor package for differential
682 expression analysis of digital gene expression data. Bioinformatics. 2010;26:139-40.
683 35. Yu G, Wang L, Han Y, He Q. ClusterProfiler: an R package for comparing biological themes
684 among gene clusters. OMICS. 2012;16:284-7.

685 36. Tsoi J, Robert L, Paraiso L, Galvan C, Sheu KM, Lay J, et al. Multi-stage differentiation
686 defines melanoma subtypes with differential vulnerability to drug-induced iron-dependent
687 oxidative stress. Cancer Cell. 2018;33:890-904.
688 37. Schaer DA, Beckmann RP, Dempsey JA, Huber L, Forest A, Amaladas N, et al. The CDK4/6
689 inhibitor abemaciclib induces a T Cell inflamed tumor microenvironment and enhances the
690 efficacy of PD-L1 checkpoint blockade. Cell Rep. 2018;22:2978–994.
691 38. Alqahtani A, Choucair K, Ashraf M, Hammouda DM, Alloghbi A, Khan T, et al. Bromodomain
692 and extra-terminal motif inhibitors: a review of preclinical and clinical advances in cancer
693 therapy. Future Sci OA. 2019;5:FSO372.
694 39. Griffiths EA, Choy G, Redkar S, Taverna P, Azab M, Karpf AR. SGI-110: DNA
695 methyltransferase inhibitor oncolytic. Drugs Future. 2013;38:535–43.
696 40. Rajapakse VN, Luna A, Yamade M, Loman L, Varma S, Sunshine M, et al. CellMinerCDB for
697 integrative cross-database genomics and pharmacogenomics analyses of cancer cell lines.
698 iScience. 2018;10:247–64.
699 41. Hofmann O, Caballero OL, Stevenson BJ, Chen Y, Cohen T, Chua R, et al. Genome-wide
700 analysis of cancer/testis gene expression. Proc Natl Acad Sci USA. 2008;105:20422-27.
701 42. Liu M, Zhang L, Li H, Hinoue T, Zhou W, Ohtani H, et al. Integrative epigenetic analysis
702 reveals therapeutic targets to the DNA methyltransferase inhibitor SGI-110 in
703 hepatocellular carcinoma. Hepatol. 2018;68:1412–428.
704 43. Subramanian A, Tamayo P, Mootha VK, Mukherjee S, Ebert BL, Gillette MA, et al. Gene set
705 enrichment analysis: a knowledge-based approach for interpreting genome-wide
706 expression profiles. Proc Natl Acad Sci USA. 2005;102:15545-50.
707 44. Ji R, Chasalow SD, Wang L, Hamid O, Schmidt H, Cogswell J, et al. An immune-active tumor
708 microenvironment favors clinical response to ipilimumab. Cancer Immunol Immunother.
709 2012;61:1019-31.

45. Hamid O, Schmidt H, Ridolfi L, Aamdal S, Hansson J, Guida M, et al. A prospective phase II trial exploring the association between tumor microenvironment biomarkers and clinical activity of ipilimumab in advanced melanoma. J Transl Med. 2011;9:204.
46. Gibbons HR, Mi DJ, Farley VM, Esmond T, Kaood MB, Aune TM. Bromodomain inhibitor JQ1 reversibly blocks IFN-γ production. Sci Rep. 2019;9:10280.
47. Gonzales-Zulueta M, Bender CM, Yang AS, Nguyen T, Beart RW, Van Tornout JM, et al. Methylation of the 5' CpG island of the p16/CDKN2 tumor suppressor gene in normal and transformed human tissues correlates with gene silencing. Cancer Res. 1995;55:4531-35.
48. Xu WS, Parmigiani RB, Marks PA. Histone deacetylase inhibitors: molecular mechanisms of action. Oncogene. 2007;26:5541–52.
49. Shi J, Vakoc CR. The mechanisms behind the therapeutic activity of BET bromodomain inhibition. Mol Cell. 2014;54:728-36.
50. Liao Y, Chen C, Shah N, Xiao T, Feit A, Yang M, et al. A non-canonical EZH2 function sensitizes solid tumors to genotoxic stress. bioRxiv. preprint doi: https://doi.org/10.1101/2020.09.11.291534.

731 **Figure legends.**

732 **Figure 1. Landscape of gene modulation by epigenetic drugs in melanoma cell lines**. Each
733 pie chart shows the % of genes significantly modulated in each of 20 families or functional groups
734 (red=upregulated genes, green=downregulated genes) by each drug in the two cell lines (VRG100
735 and CST30), on the basis of FC and p value. The 20 gene families are further classified into 7
736 groups identified on the right hand side of the figure: 1, epigenetic regulation; 2, proliferation; 3,
737 immune regulation; 4, enzymes; 5, structural components; 6, adhesion; 7, differentiation.

738 **Figure 2. Immune-related gene modulation by epigenetic drugs in melanoma**.
739 Modulation of 731 genes was assessed by the Nanostring Cancer Immune panel upon treatment
740 with 4 epigenetic drugs and with Abemaciclib of ten melanoma cell lines with the indicated
741 mutational and differentiation profiles (as defined in Tables S1 and Fig. S2, respectively). Genes in
742 the Nanostring panel were grouped into 21 functional classes (as described in Fig. S7). The overall
743 modulatory activity of all drugs on each gene class was visualized by *ad-hoc* developed, color-
744 coded metrics described at the bottom of the Figure. The first metric adopts a red/green color
745 code to visualize instances of predominant up- or down-regulation of genes by each drug and in
746 each cell line. This metric contains a normalization factor (=[(%UP+%DN)/100)]) that takes into
747 account the different number of genes modulated in each cell line. The second metrics adopts
748 shades of blue to visualize instances where an equal fraction of up- and down-modulated genes in
749 each class was observed. Up- or down-modulation of each gene by any drug was defined on the
750 basis of a Treated/Control ratio >|1.5|. *: these two cell lines were treated with decitabine, the
751 active metabolite of guadecitabine.

752 **Figure 3. Quantitative western blot analysis for modulation of immune-related proteins**
753 **in melanoma cell lines by epigenetic drugs.** Eleven melanoma cell lines were treated with
754 guadecitabine (GUA), givinostat (GIV), JQ1, OTX-015 (OTX), GSK-126 (GSK) and abemaciclib

(ABEMA) and assessed for expression/modulation of 14 proteins. Modulation of each protein by drug treatment, based on data analysis and visualization approach described in Fig. S15 and S16, is visualized by a color code shown at the bottom of the figure. Grey boxes: the antigen was not expressed and not induced by treatments.

Figure 4. Guadecitabine is an activator of innate immunity and inflammation pathways. **A.** Upstream Regulators predicted to be activated (Z score >2, p value <0.05, left graph) or inhibited (Z score <-2, p value <0.05, right graph), in at least 6/10 cell lines. **B**. Upstream Regulators predicted to be activated (Z score >2, p value <0.05) in 5/10 cell lines. Data in A and B based on IPA analysis of Nanostring gene modulation data. Color-coded arrows define the biological function/pathway of each UR. Each black dot in the two graphs represents the Z score value of the indicated URs, computed for a single cell line.

Figure 5. Comparison of Upstream Regulators activated by guadecitabine in melanoma vs mesothelioma and in melanoma vs hepatocarcinoma cell lines. **A, B**. Scatter plot of URs activated by guadecitabine in melanoma vs mesothelioma (A) and in melanoma vs hepatocarcinoma cell lines (B, according to gene expression data retrieved from ref. 42). Guadecitabine UR signature molecules shown in this figure are highlighted with the same color code used in Fig. 4 to mark the biological function/pathway. *: identity of URs shown in the square in panel A.

Figure 6. Expression and modulation of guadecitabine-specific signature genes in baseline and on-treatment clinical samples from NIBIT-M4 patients. **A**. Heatmap of log2 fold changes of guadecitabine signature genes among the following comparisons: w4 vs. w0, w12 vs. w4 and w12 vs w0. **B-D**. Enrichment plots containing profiles of the running enrichment scores (ES) and positions of guadecitabine gene set members on the rank ordered list in GSEA for w4 vs. w0 (B), w12 vs. w4 (C) and w12 vs. w0 (D) comparisons.

Figure 7. Activation of guadecitabine-specific UR signature molecules in on-treatment tumor biopsies from responding compared to non-responding patients in the NIBIT-M4 trial. A, B. Z score values of guadecitabine-activated URs as identified in Fig. 4A (A) or in Fig. 4B (B) based on differential gene expression analysis in tumor samples (obtained at w0, w4 and w12) from responding (n=3) vs non-responding patients (n=5). Only significant URs (Z score >2) are shown by the indicated color code. **C**. Scatter plot of Z score values of activated URs in responding vs non-responding patients at w4 vs. wk12.

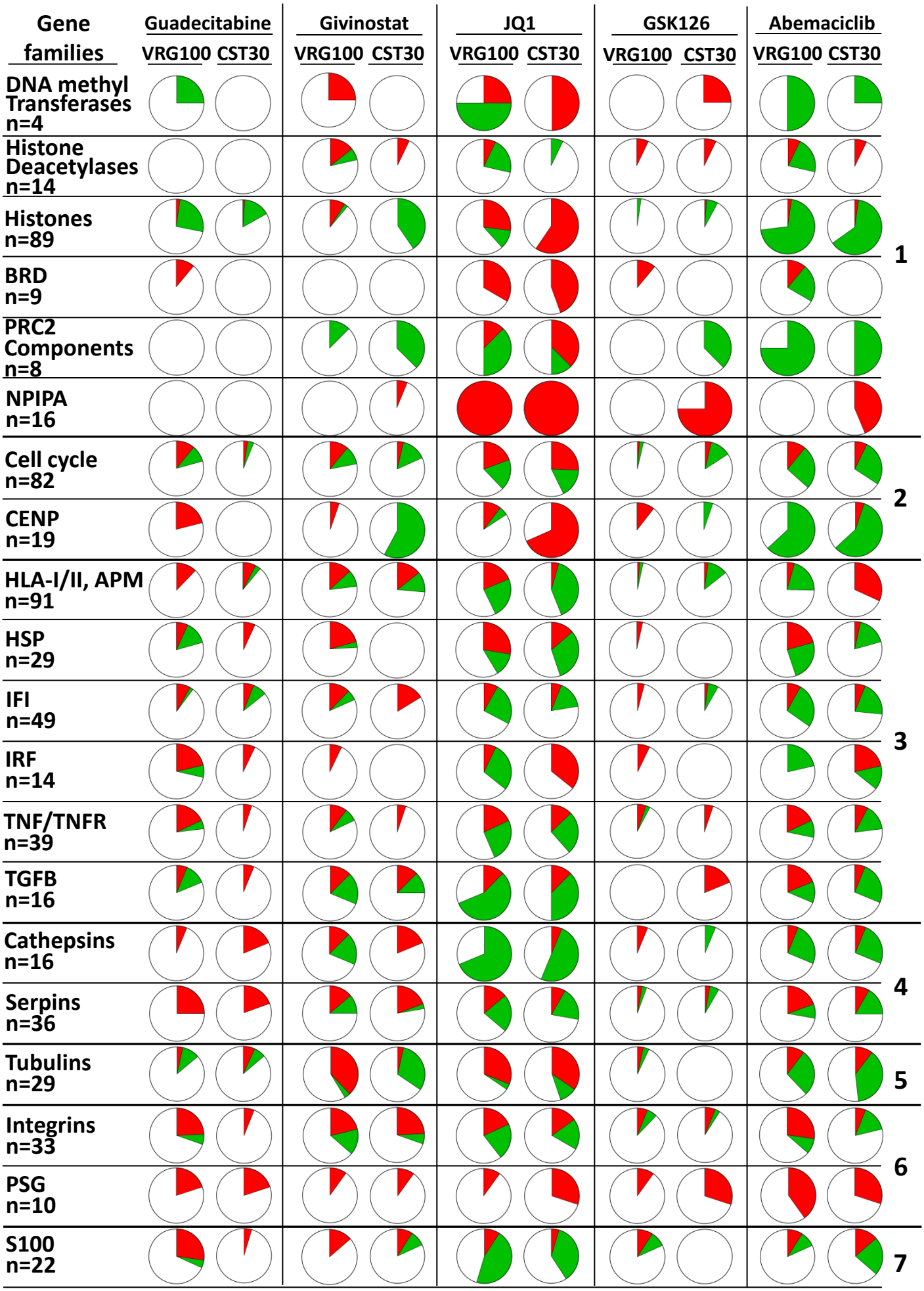
Gene families
Guadecitabine
VRG100 CST30
Givinostat
VRG100 CST30
JQ1
VRG100 CST30
GSK126
VRG100 CST30
Abemaciclib
VRG100 CST30
DNA methyl Transferases n=4
Histone Deacetylases n=14
Histones n=89
BRD n=9
PRC2 Components n=8
NPIPA n=16
Cell cycle n=82
CENP n=19
HLA-I/II, APM n=91
HSP n=29
IFI n=49
IRF n=14
TNF/TNFR n=39
TGFB n=16
Cathepsins n=16
Serpins n=36
Tubulins n=29
Integrins n=33
PSG n=10
S100 n=22
1
2
3
4
5
6
7

Figure 2

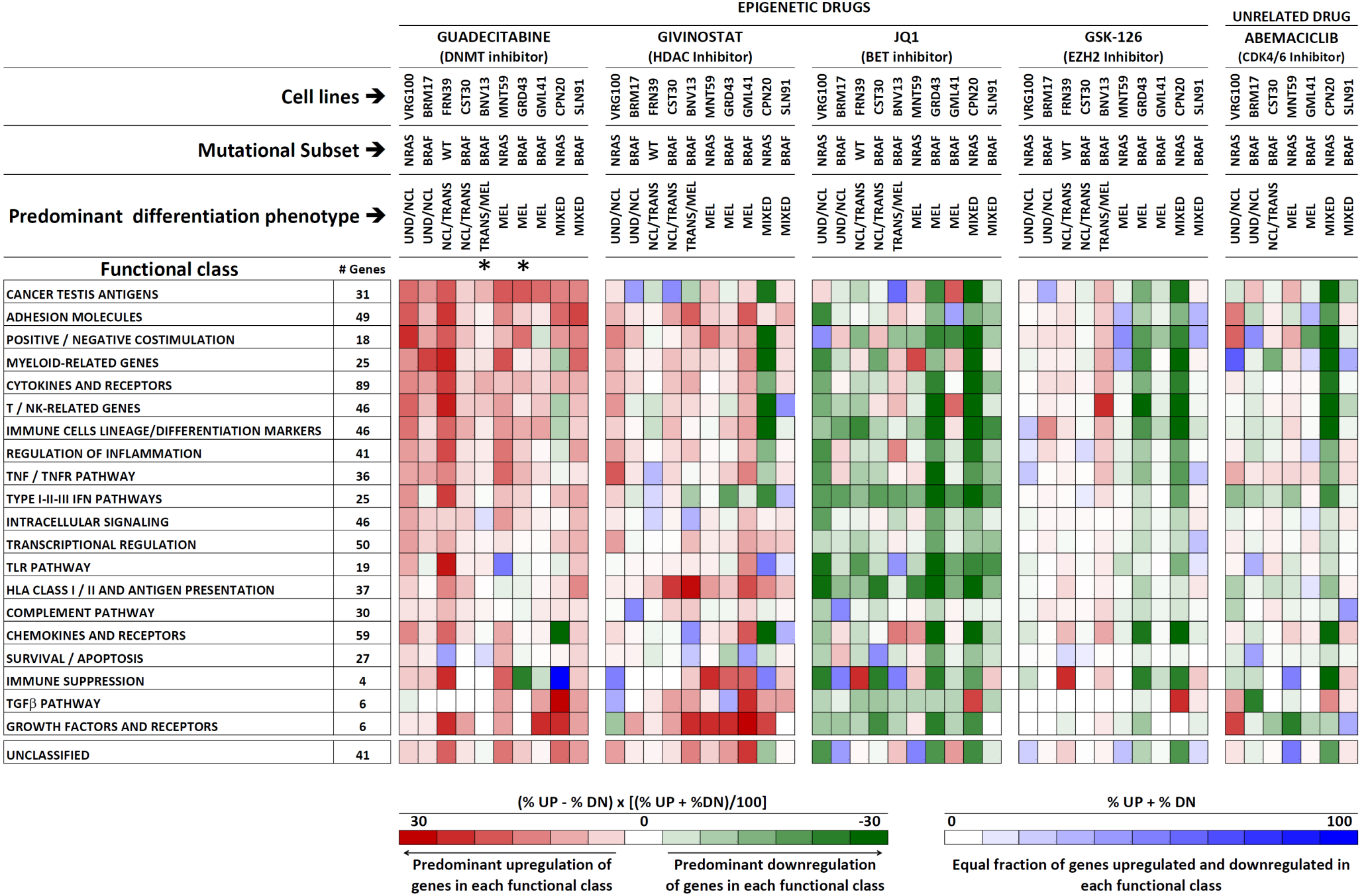
EPIGENETIC DRUGS
UNRELATED DRUG
GUADECITABINE
(DNMT inhibitor)
GIVINOSTAT
(HDAC Inhibitor)
JQ1
(BET inhibitor)
GSK-126
(EZH2 Inhibitor)
ABEMACICLIB
(CDK4/6 Inhibitor)
Cell lines
Mutational Subset
Predominant differentiation phenotype
VRG100 BRM17 FRN39 CST30 BNV13 MNT59 GRD43 GML41 CPN20 SLN91
NRAS BRAF WT BRAF BRAF NRAS BRAF BRAF NRAS BRAF
UND/NCL UND/NCL NCL/TRANS NCL/TRANS TRANS/MEL MEL MEL MEL MIXED MIXED
VRG100 BRM17 CST30 MNT59 GML41 CPN20 SLN91
NRAS BRAF BRAF NRAS BRAF NRAS BRAF
UND/NCL UND/NCL NCL/TRANS MEL MEL MIXED MIXED
Functional class
Genes
CANCER TESTIS ANTIGENS 31
ADHESION MOLECULES 49
POSITIVE / NEGATIVE COSTIMULATION 18
MYELOID-RELATED GENES 25
CYTOKINES AND RECEPTORS 89
T / NK-RELATED GENES 46
IMMUNE CELLS LINEAGE/DIFFERENTIATION MARKERS 46
REGULATION OF INFLAMMATION 41
TNF / TNFR PATHWAY 36
TYPE I-II-III IFN PATHWAYS 25
INTRACELLULAR SIGNALING 46
TRANSCRIPTIONAL REGULATION 50
TLR PATHWAY 19
HLA CLASS I / II AND ANTIGEN PRESENTATION 37
COMPLEMENT PATHWAY 30
CHEMOKINES AND RECEPTORS 59
SURVIVAL / APOPTOSIS 27
IMMUNE SUPPRESSION 4
TGFβ PATHWAY 6
GROWTH FACTORS AND RECEPTORS 6
UNCLASSIFIED 41
(% UP - % DN) x [(% UP + %DN)/100]
30
0
-30
Predominant upregulation of genes in each functional class
Predominant downregulation of genes in each functional class
% UP + % DN
0
100
Equal fraction of genes upregulated and downregulated in each functional class

Figure 3

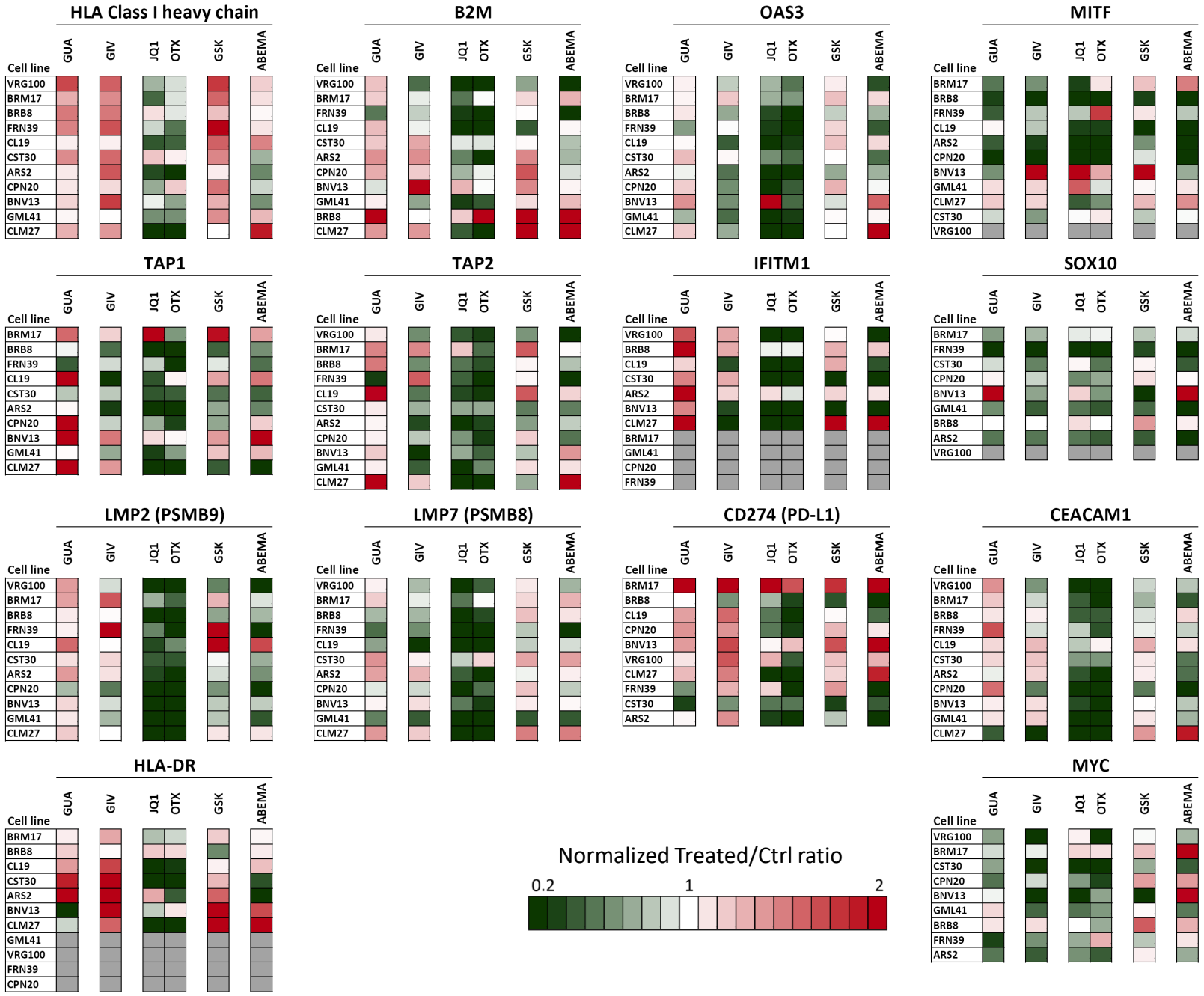
HLA Class I heavy chain
B2M
OAS3
MITF
TAP1
TAP2
IFITM1
SOX10
LMP2 (PSMB9)
LMP7 (PSMB8)
CD274 (PD-L1)
CEACAM1
HLA-DR
MYC
Cell line
GUA
GIV
JQ1
OTX
GSK
ABEMA
Normalized Treated/Ctrl ratio
0.2
1
2

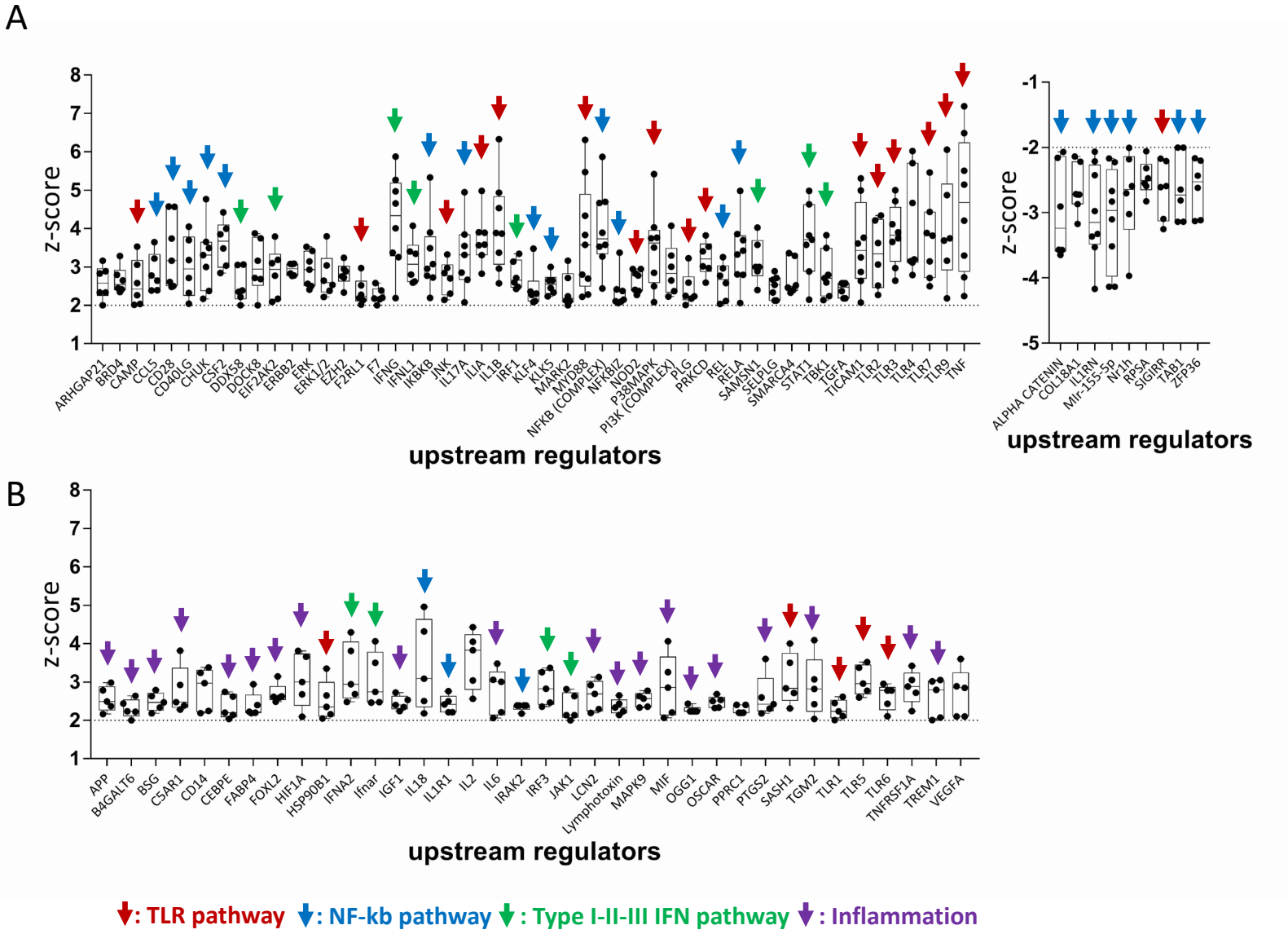
A
z-score
upstream regulators
ARHGAP21 BRD4 CAMP CCL5 CD28 CD40LG CHUK CSF2 DDX58 DOCK8 EIF2AK2 ERBB2 ERK ERK1/2 EZH2 F2RL1 F7 IFNG IFNL1 IKBKB JNK IL17A IL1A IL1B IRF1 KLF4 KLK5 MARK2 MYD88 NFKB (COMPLEX) NFKBIZ NOD2 P38MAPK PI3K (COMPLEX) PLG PRKCD REL RELA SAMSN1 SELPLG SMARCA4 STAT1 TBK1 TGFA TICAM1 TLR2 TLR3 TLR4 TLR7 TLR9 TNF
ALPHA CATENIN COL18A1 IL1RN Mir-155-5p Nr1h RPSA SIGIRR TAB1 ZFP36
B
APP B4GALT6 BSG C5AR1 CD14 CEBPE FABP4 FOXL2 HIF1A HSP90B1 IFNA2 Ifnar IGF1 IL18 IL1R1 IL2 IL6 IRAK2 IRF3 JAK1 LCN2 Lymphotoxin MAPK9 MIF OGG1 OSCAR PPRC1 PTGS2 SASH1 TGM2 TLR1 TLR5 TLR6 TNFRSF1A TREM1 VEGFA
: TLR pathway : NF-kb pathway : Type I-II-III IFN pathway : Inflammation

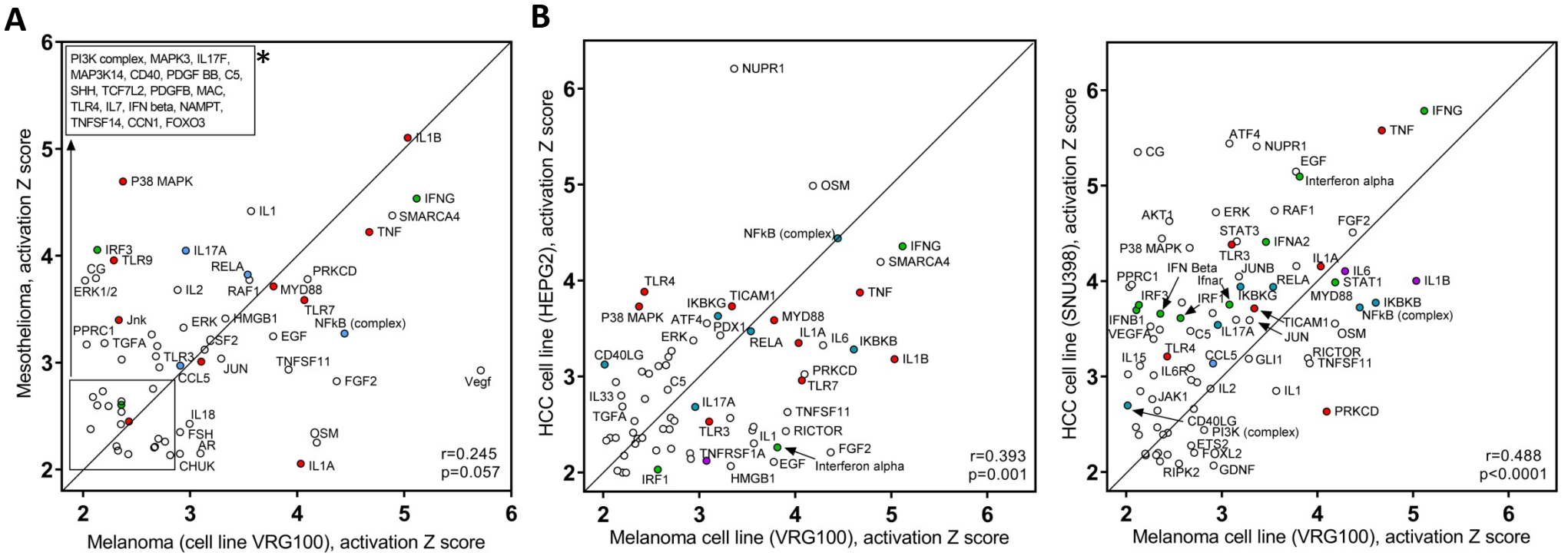
A
PI3K complex, MAPK3, IL17F, MAP3K14, CD40, PDGF BB, C5, SHH, TCF7L2, PDGFB, MAC, TLR4, IL7, IFN beta, NAMPT, TNFSF14, CCN1, FOXO3
*
Mesothelioma, activation Z score
Melanoma (cell line VRG100), activation Z score
r=0.245
p=0.057
IL1B
P38 MAPK
IFNG
IL1
SMARCA4
TNF
IRF3
IL17A
TLR9
RELA
CG
PRKCD
ERK1/2
IL2
RAF1
MYD88
TLR7
Jnk
ERK
HMGB1
NFkB (complex)
PPRC1
TGFA
EGF
CSF2
TLR3
TNFSF11
JUN
CCL5
FGF2
Vegf
IL18
FSH
OSM
AR
CHUK
IL1A
B
HCC cell line (HEPG2), activation Z score
Melanoma cell line (VRG100), activation Z score
r=0.393
p=0.001
NUPR1
OSM
NFkB (complex)
IFNG
SMARCA4
TLR4
TICAM1
TNF
IKBKG
P38 MAPK
ATF4
PDX1
MYD88
ERK
RELA
IL1A
IL6
IKBKB
CD40LG
IL1B
PRKCD
C5
TLR7
IL33
IL17A
TNFSF11
TGFA
TLR3
IL1
RICTOR
TNFRSF1A
FGF2
EGF
Interferon alpha
IRF1
HMGB1
C
HCC cell line (SNU398), activation Z score
Melanoma cell line (VRG100), activation Z score
r=0.488
p<0.0001
IFNG
TNF
ATF4
NUPR1
CG
EGF
Interferon alpha
AKT1
ERK
RAF1
FGF2
STAT3
IFNA2
P38 MAPK
TLR3
IL1A
IFN Beta
JUNB
IL6
PPRC1
Ifnar
RELA
STAT1
IL1B
IRF3
IRF1
IKBKG
MYD88
IKBKB
IFNB1
TICAM1
NFkB (complex)
VEGFA
C5
IL17A
JUN
OSM
IL15
TLR4
CCL5
GLI1
RICTOR
TNFSF11
IL6R
IL2
IL1
JAK1
PRKCD
CD40LG
PI3K (complex)
ETS2
FOXL2
RIPK2
GDNF

Figure 6

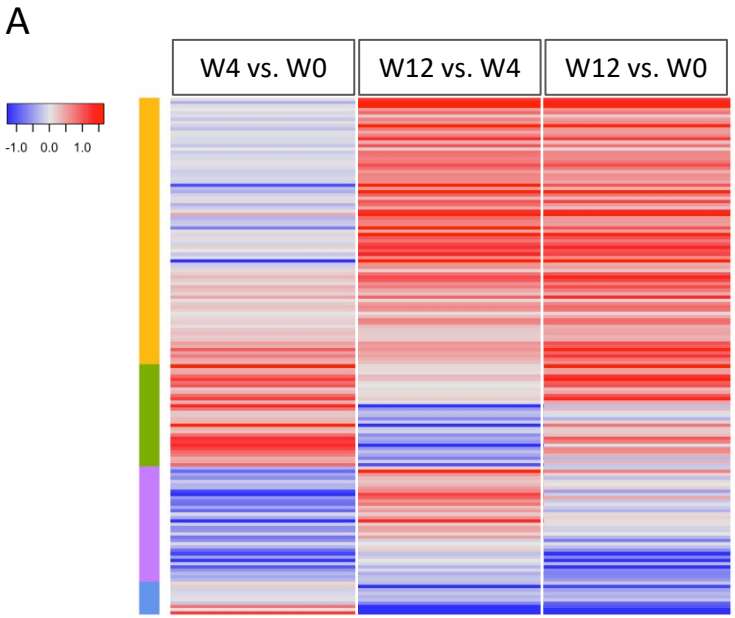
A
W4 vs. W0
W12 vs. W4
W12 vs. W0
-1.0 0.0 1.0

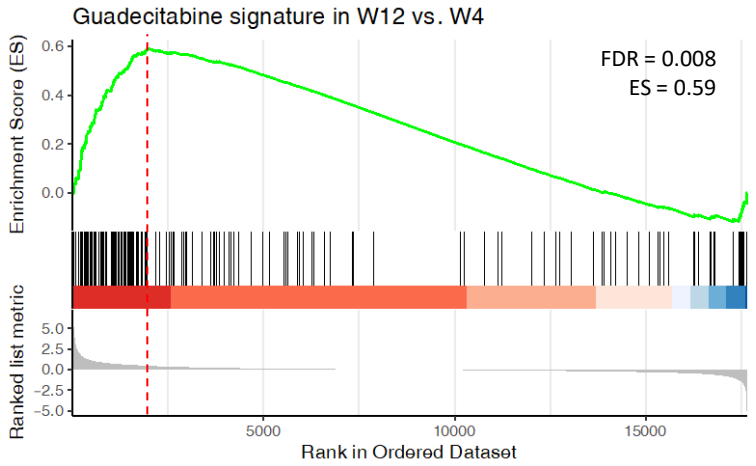
C
Guadecitabine signature in W12 vs. W4
FDR = 0.008
ES = 0.59
Enrichment Score (ES)
Ranked list metric
Rank in Ordered Dataset

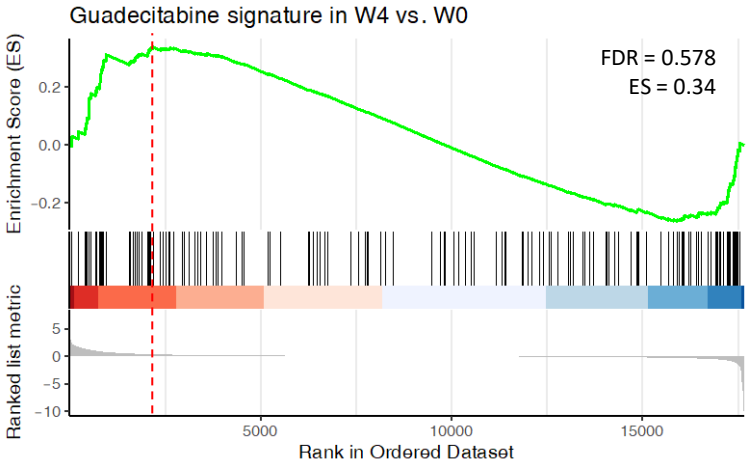
B
Guadecitabine signature in W4 vs. W0
FDR = 0.578
ES = 0.34
Enrichment Score (ES)
Ranked list metric
Rank in Ordered Dataset

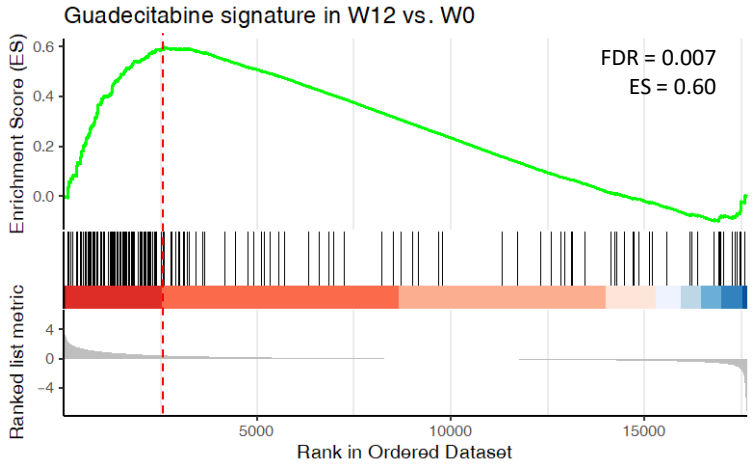
D
Guadecitabine signature in W12 vs. W0
FDR = 0.007
ES = 0.60
Enrichment Score (ES)
Ranked list metric
Rank in Ordered Dataset

Figure 7

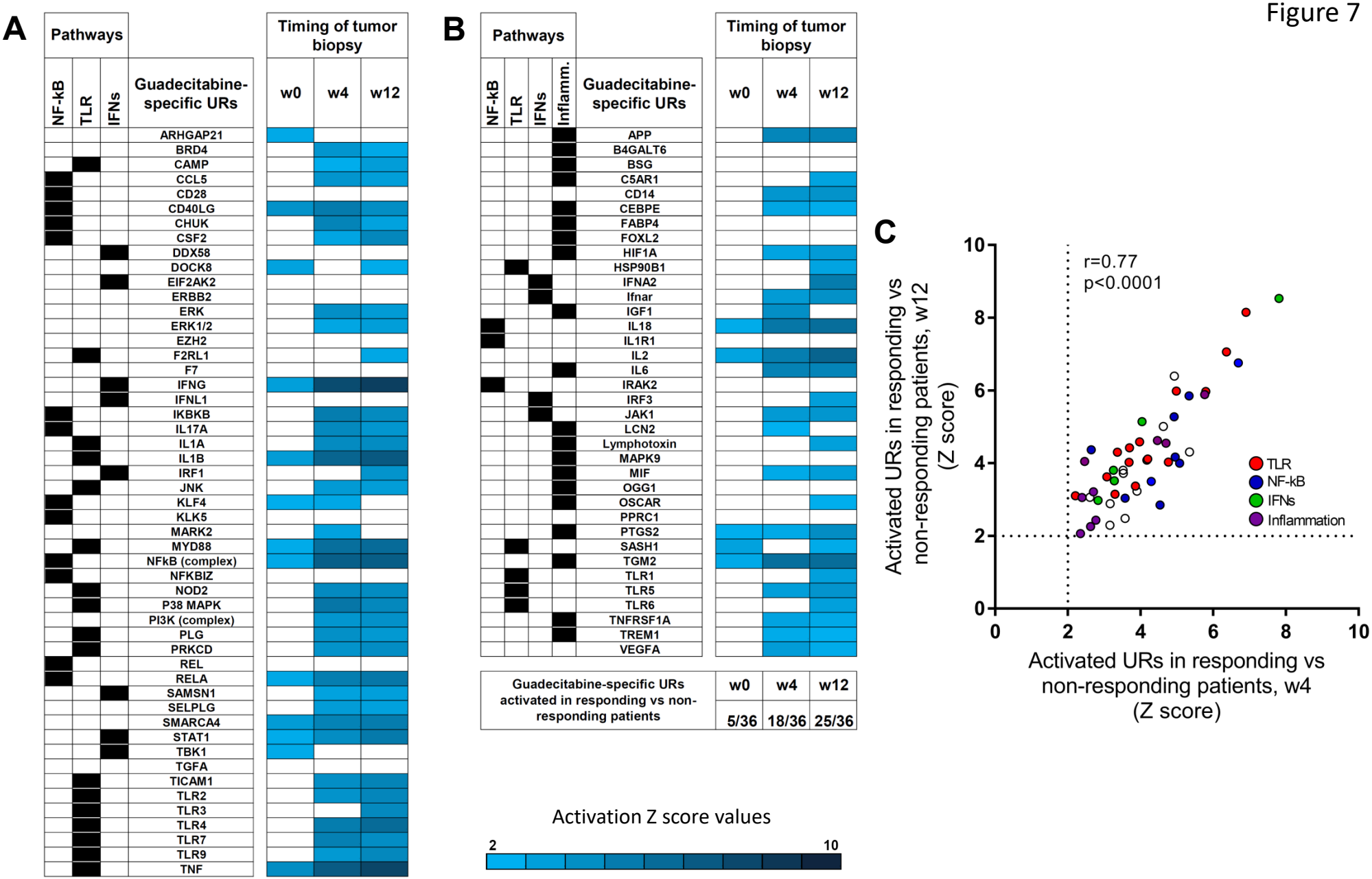
A
Pathways
NF-kB
TLR
IFNs
Guadecitabine-specific URs
Timing of tumor biopsy
w0
w4
w12
ARHGAP21
BRD4
CAMP
CCL5
CD28
CD40LG
CHUK
CSF2
DDX58
DOCK8
EIF2AK2
ERBB2
ERK
ERK1/2
EZH2
F2RL1
F7
IFNG
IFNL1
IKBKB
IL17A
IL1A
IL1B
IRF1
JNK
KLF4
KLK5
MARK2
MYD88
NFkB (complex)
NFKBIZ
NOD2
P38 MAPK
PI3K (complex)
PLG
PRKCD
REL
RELA
SAMSN1
SELPLG
SMARCA4
STAT1
TBK1
TGFA
TICAM1
TLR2
TLR3
TLR4
TLR7
TLR9
TNF
Guadecitabine-specific URs activated in responding vs non-responding patients
w0 13/51
w4 34/51
w12 36/51
B
Pathways
NF-kB
TLR
IFNs
Inflamm.
Guadecitabine-specific URs
Timing of tumor biopsy
w0
w4
w12
APP
B4GALT6
BSG
C5AR1
CD14
CEBPE
FABP4
FOXL2
HIF1A
HSP90B1
IFNA2
Ifnar
IGF1
IL18
IL1R1
IL2
IL6
IRAK2
IRF3
JAK1
LCN2
Lymphotoxin
MAPK9
MIF
OGG1
OSCAR
PPRC1
PTGS2
SASH1
TGM2
TLR1
TLR5
TLR6
TNFRSF1A
TREM1
VEGFA
Guadecitabine-specific URs activated in responding vs non-responding patients
w0 5/36
w4 18/36
w12 25/36
Activation Z score values
2
10
C
r=0.77
p<0.0001
Activated URs in responding vs non-responding patients, w12 (Z score)
Activated URs in responding vs non-responding patients, w4 (Z score)
TLR
NF-kB
IFNs
Inflammation
0
2
4
6
8
10